Antiferromagnetic Ordering in the S=1 Quasi-One-Dimensional $PbNi_{2-x}Mg_xV_2O_8$ (x=0.24)

V. Pomjakushin

I.M.Frank Laboratory of Neutron Physics, JINR , Dubna

In collaboration with:

A. Lappas and J. Giapintzakis

Institute of Electronic Structure and Laser, Heraklion – Crete, Greece

Thanks to:

L.Keller, P.Fischer (LNS PSI/ETHZ)
and A.Schenck (IPP/PSI)

1D quantum Heisenberg AF

$$H = -J\sum_i \mathbf{S}_i\mathbf{S}_{i+1} + D\sum_i (S_i^z)^2$$

F.D.M.Haldane, *PRL.* **50,** 1153 (1983)

I. Affleck et al, *PRL* **59**, 799 (1987)

▪S=1/2 (or half-odd-integer)

Continuum excitation spectrum E(k)

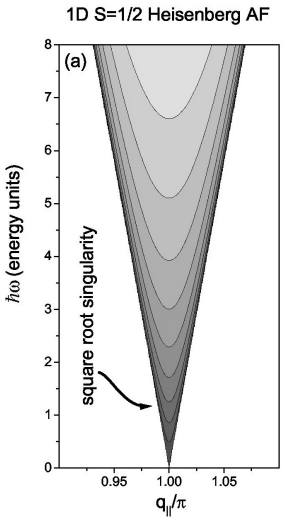

e.g. good 1D:
Sr_2CuO_3, Sr_2CuO_3

▪Arbitrary weak interchain J_1suppress QF :
$T_N \sim J_1$, $\mu \sim J_1/J$
e.g. $SrCuF_3$ $T_N \approx 40K$,
$\mu \approx 0.5\ \mu_B$

The spin-½ dimerized Valence Bond states

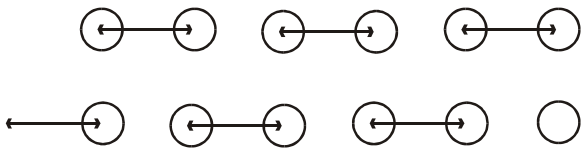

▪Ground state is **Resonating Valence Bond /RVB:**
QF restore translational symmetry and mix in bounds of greater length

▪S=1 (or integer)

$E(k)=[v^2(k-\pi)^2+\Delta^2]^{1/2}$

Haldane gap $\Delta \sim 2Je^{-\pi S}$

Singlet ground state

▪The spin-1**Valence Bond Solid /VBS**

$e_0=-4/3J$

The spin-1 dimerized states

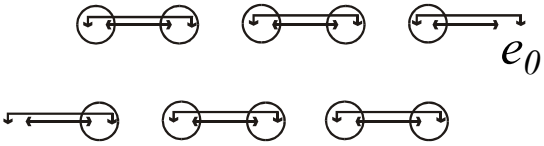

$e_0=- -J$

ESR in Cu^{2+}/Ni^2 substituted $[Ni(C_2H_8N_2)_2(NO_2)]ClO_4$ (NENP) shows spin-½ end states → **VBS**

▪Energetics of a Haldane gap AF

from MC calculations

$\Delta_{xx} \approx \Delta - (2/3)D$; $\Delta_{zz} \approx \Delta + (4/3)D$

$\Delta = 0.41J$; $v = 2.49J$; $\xi = 2J/\Delta \sim 5$

$E_0 = e_0 + A\ exp(-L/\xi)$; $e_0 = -1.4J$

Long range order in a Haldane-gap S=1 quasi 1D-AFM

$$H = -J\sum_i \mathbf{S}_i\mathbf{S}_{i+1} + D\sum_i (S_i^z)^2 - J_1 \sum_{i\text{nterchain}} \mathbf{S}_i\mathbf{S}_{i+1}$$

- Interchain interactions J' and ion anisotropy D promote LRO /Phase diagram from T.Sakai, M.Takahashi PRB **42**, 4537 (1990); A.Zheludev et al., PRB **62**, 8921 (2000)./

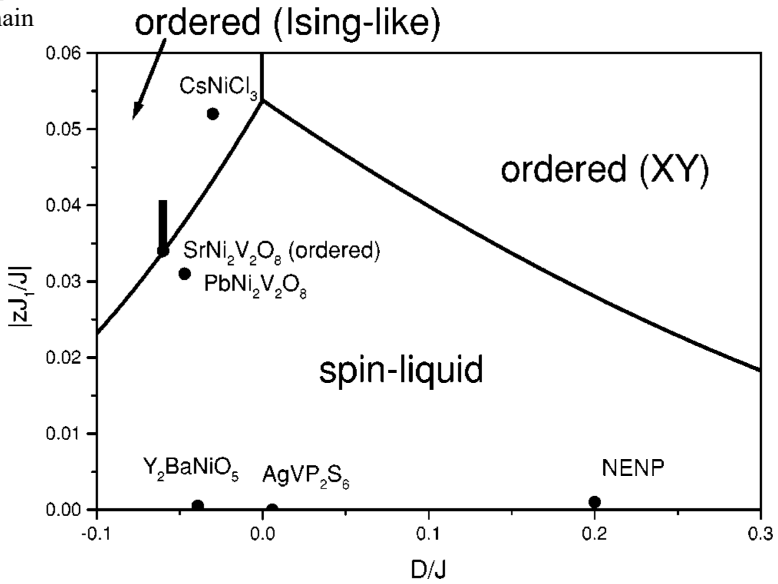

- External magnetic field suppress QF, restore gapless spectrum. $Ni(C_5D_{14}N_2)_2N_3(PF_6)$ /NDMAP/ (Pnmn, chains along c) LRO AFM at >5T /Y.Chen et al., Phys. Rev. Lett. 86, 1618 (2001)

- **Spin-vacancy induced LRO** /Theoretically suggested: E.F. Shender and S.A. Kivelson, *Phys. Rev. Lett.* **66**. 2384 (1991) /

Experimentally observed only in $PbMg_{2-x}A_xV_2O_8$
/Y. Uchiyama, et al, *PRL* **83**, 632 (1999); Physica B**284-288**, 1641 (2000)/

Energetics of $PbMg_2V_2O_8$

Δ_{zz}=35K, Δ_{xx}=46K, J=-95K, J_1=-2K

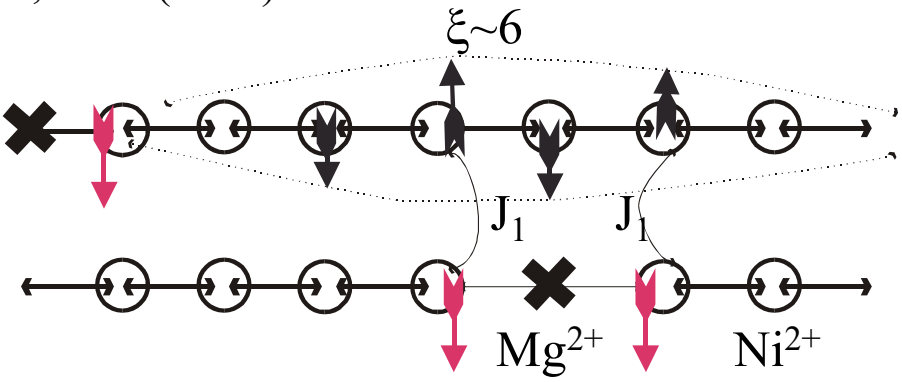

Crystal structure of $PbNi_2V_2O_8$

a tetragonal crystal structure (a=b=12.2 Å, c=8.4 Å, space group $I4_1cd$) isomorphous to $SrNi_2V_2O_8$

(a)

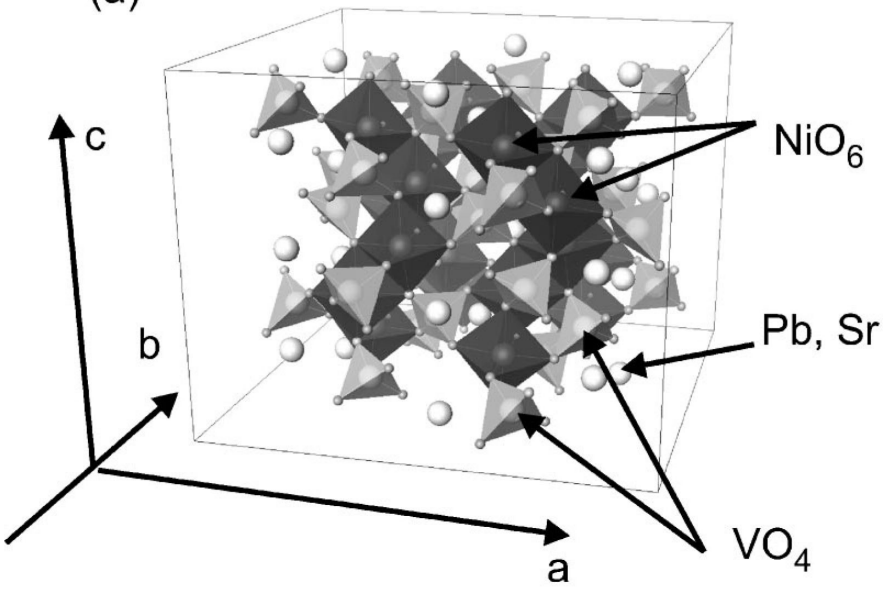

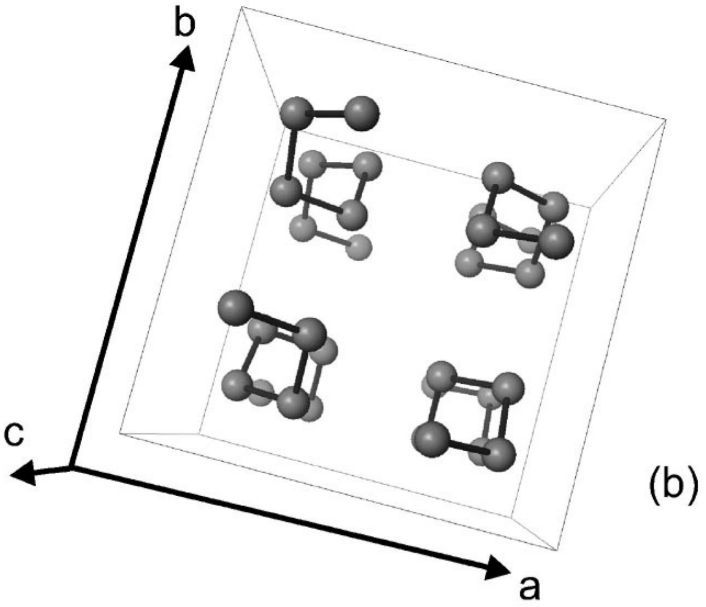

(b)

Ni-Ni distances

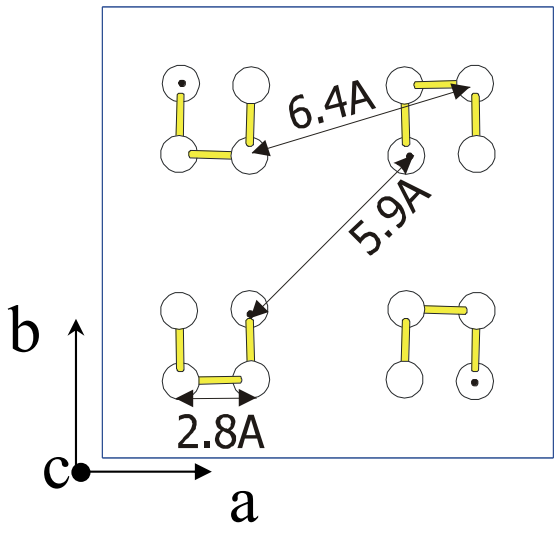

χ_{dc}(T) and *T*-*x* phase diagram of $PbNi_{2-x}Mg_xV_2O_8$

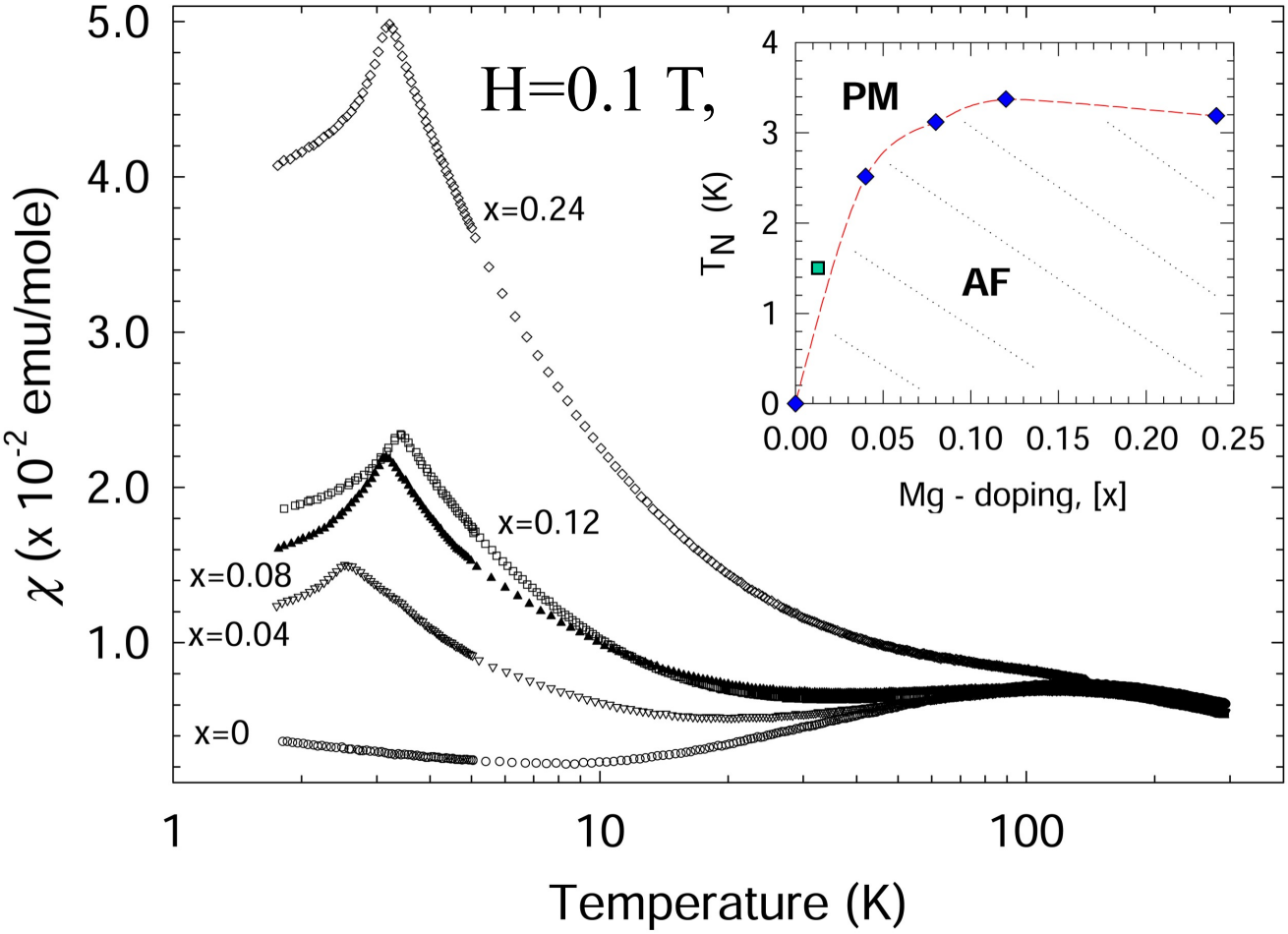

- Low-T (6<T<40K):
  $\chi(T) \cong \chi(0) + C\, e^{-\Delta/kT}$, $\Delta \cong$HaldaneGap =30.2(2) K.*
- High-T (160<T<300 K):
  $\chi_{dc}(T) = N(g\mu)^2/kT\, f(J/T)$ "a series expansion for a *S*=1 1D-HAF"
  → J=-90.4(3) K*. $\Delta / |J| = 0.31$

*In accord with Y. Uchiyama, et al, *Phys. Rev. Lett.* **83**, 632 (1999)

Suppressing of the AF transition by external magnetic field

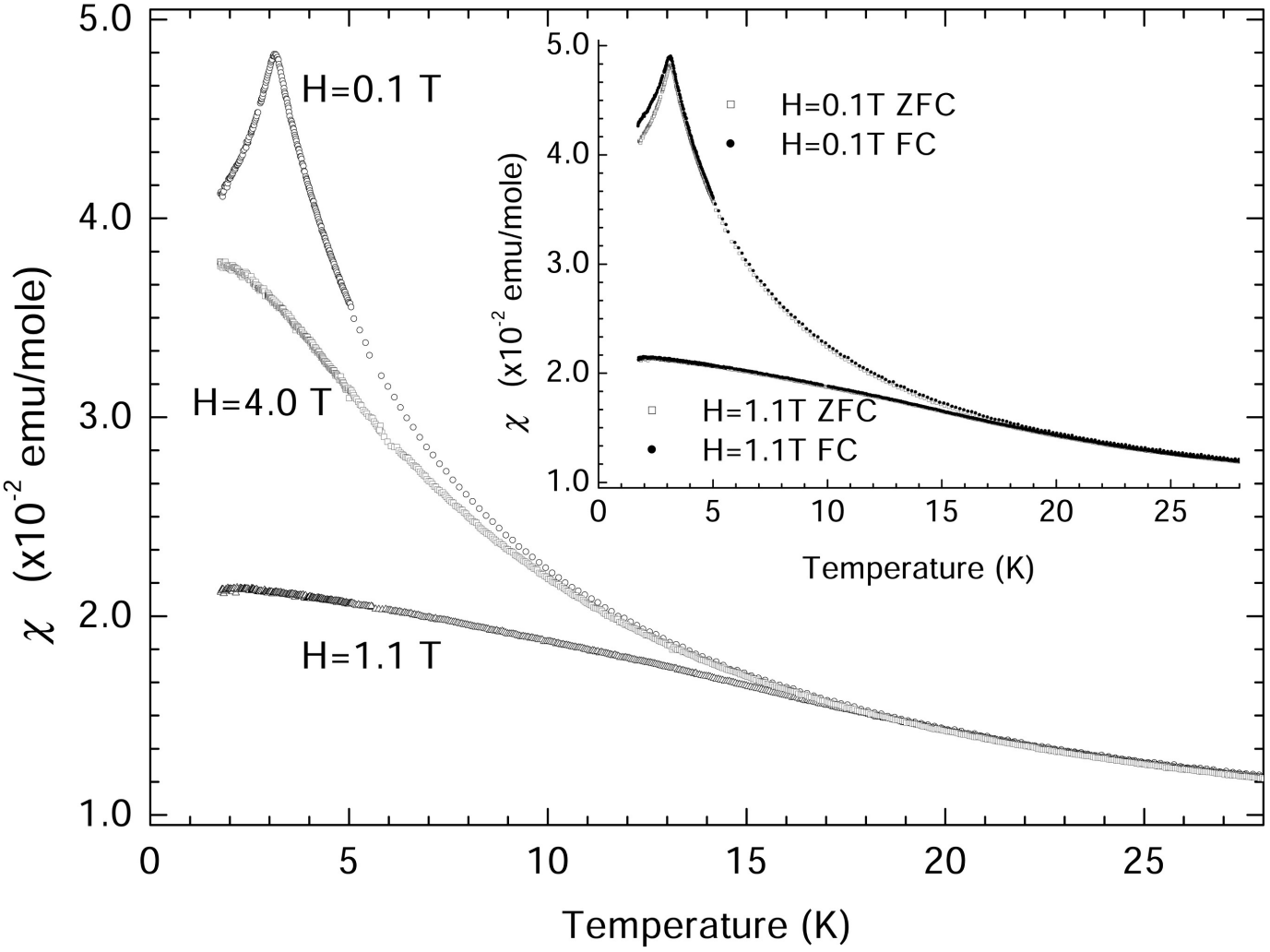

Temperature dependence of the dc susceptibility of $PbNi_{1.76}Mg_{0.24}V_2O_8$ for ZFC conditions in different magnetic fields. *Inset*: χ_{dc} vs. T, measured under ZFC and FC conditions in 0.1 and 1.1 Tesla.

Metamagnetic behaviour of $PbNi_{2-x}Mg_xV_2O_8$ (x=0.24)

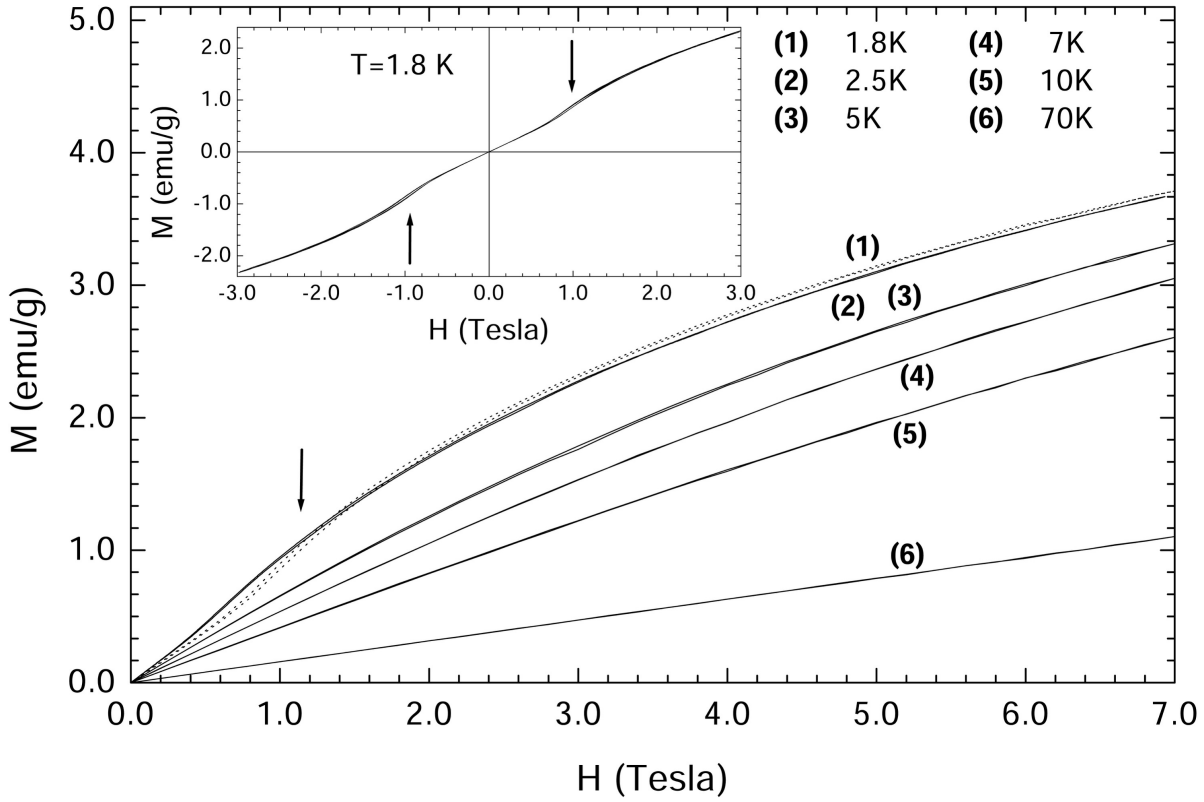

Magnetisation, *M* as a function of the applied magnetic field, *H* for various temperatures above and below T_N=3.2K. *Inset*: Full hysteresis loop for *T*=1.8K.

H-T phase diagram of $PbNi_{2-x}Mg_xV_2O_8$ (x=0.24)

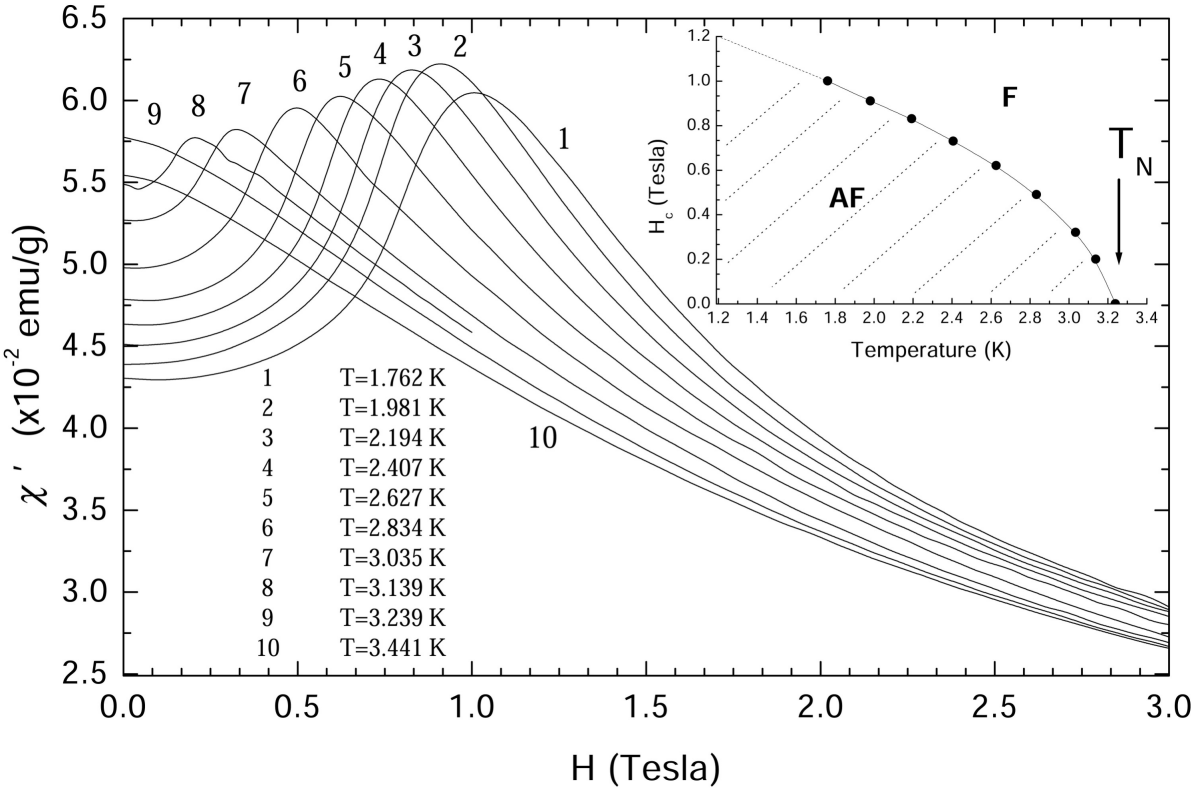

Dc magnetic field (*H*) dependence of the real part of the ac susceptibility, χ'(H), measured (h_{ac}=1 Oe, f=1 kHz) at several temperatures below T_N. *Inset*: Phase diagram in the *H-T* plane.

Neutron diffraction pattern. Crystal structure.

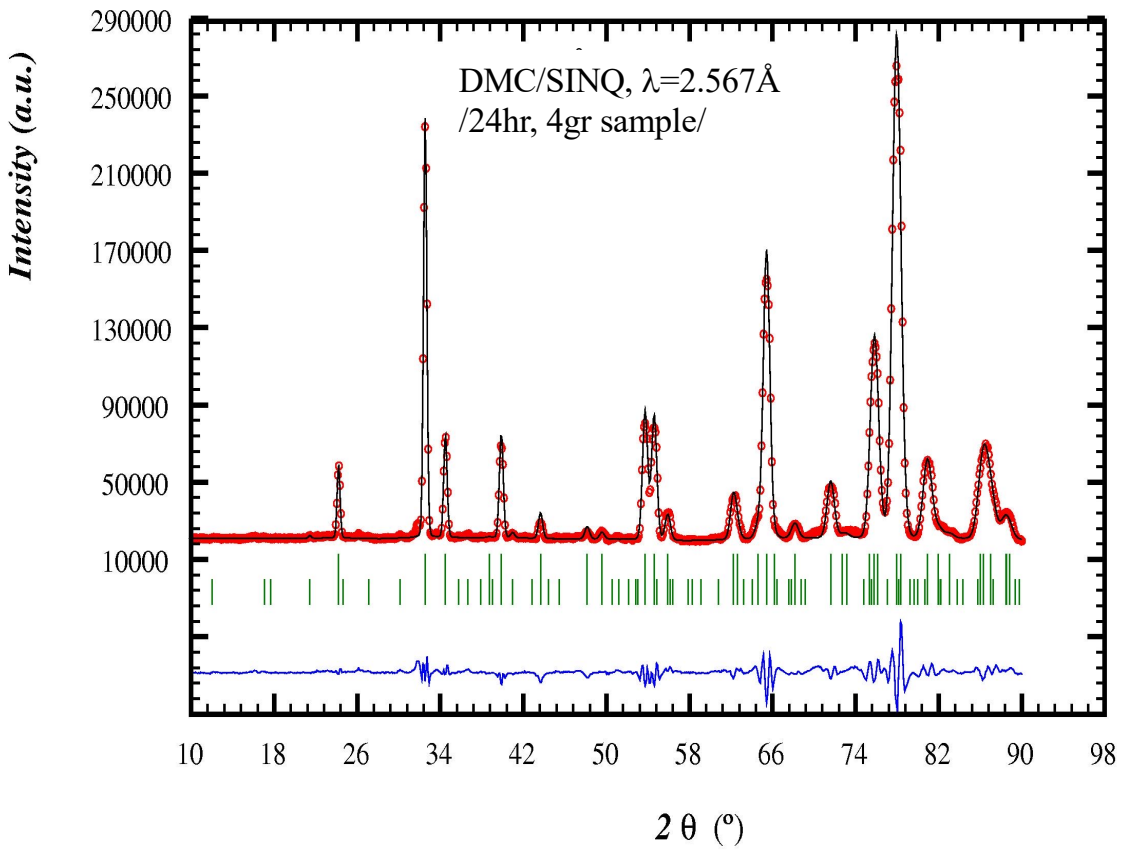

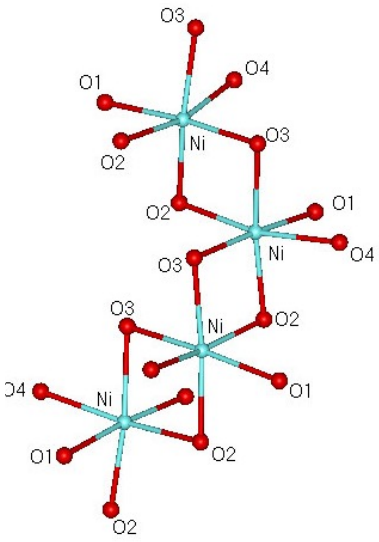

	site	*x*	*y*	*z*
Pb	8a	0	0	0
Ni	16b	0.3262(9)	0.3303(7)	0.1714(14)
Mg	16b	0.3262(9)	0.3303(7)	0.1714(14)
V	16b	0.2578	0.0797	0.1011
O(1)	16b	0.155(1)	0.495(2)	-0.097(2)
O(2)	16b	0.338(2)	0.655(1)	0.434(2)
O(3)	16b	0.161(2)	0.689(1)	0.671(2)
O(4)	16b	0.330(1)	0.499(1)	0.199(2)
Space group: $I4_1cd$. $a=b=$ 12.2448(7) Å, $c=$ 8.3592(7) Å				

$PbNi_{2-x}Mg_xV_2O_8$ (x=0.24), DMC λ=2.567Å

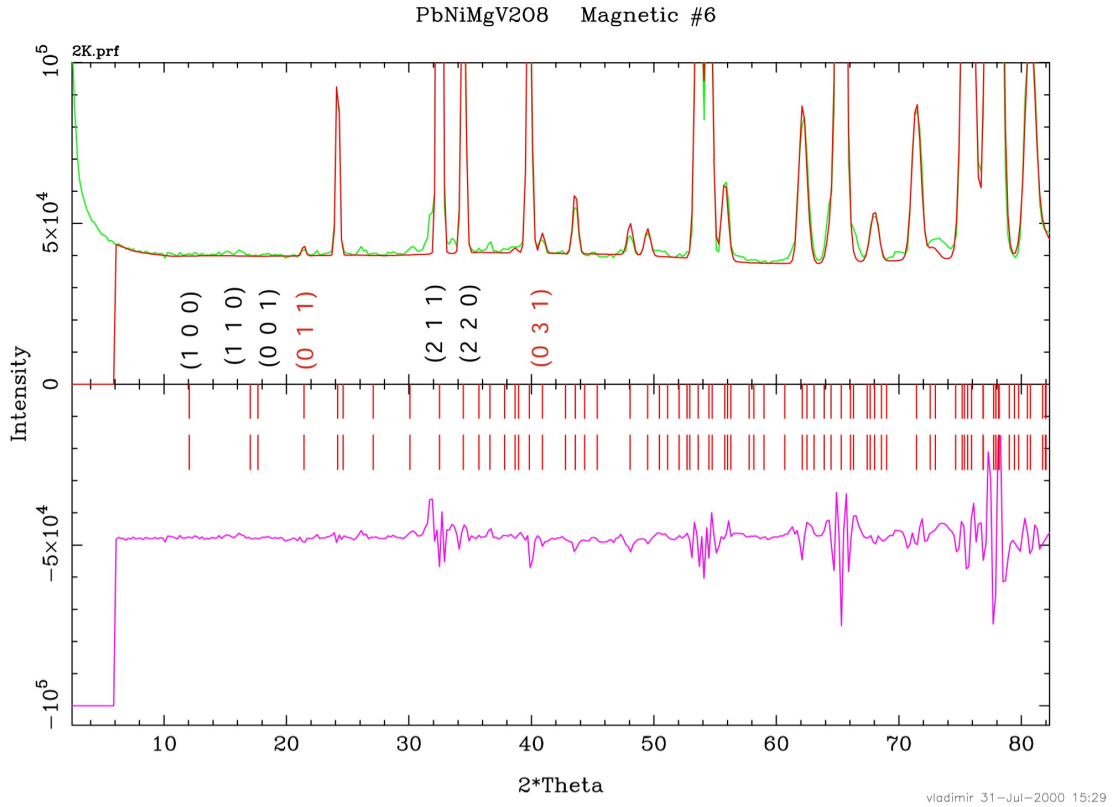

T=2K

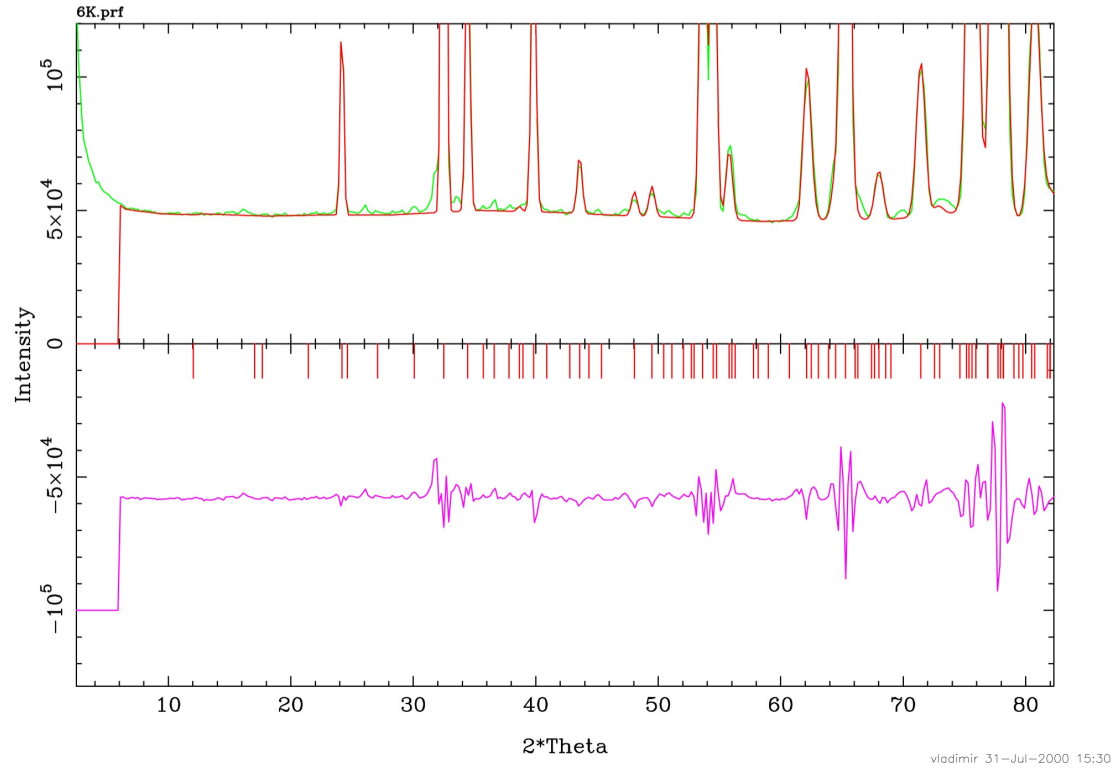

T=4K

Difference pattern “2K-4K”

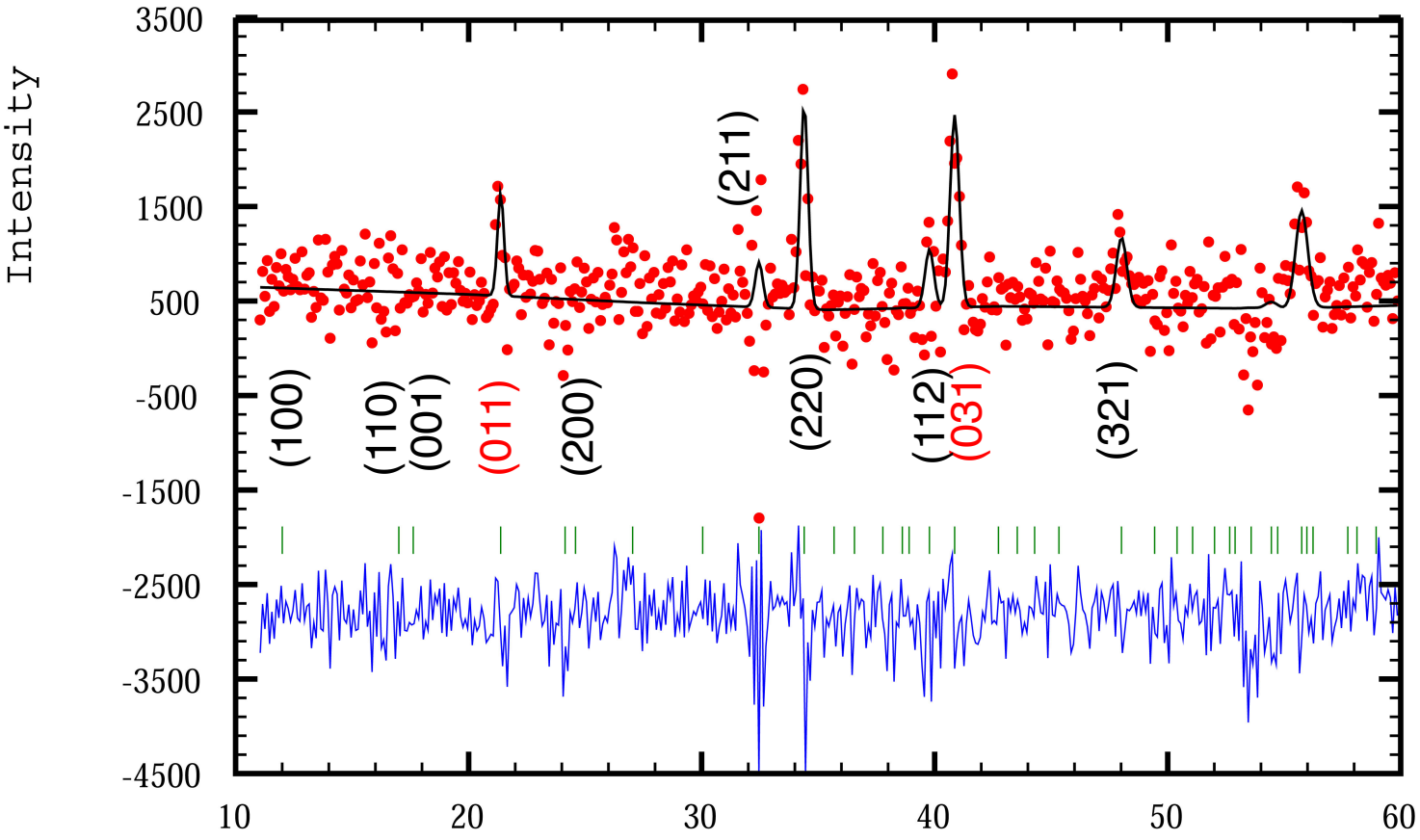

k=0

h+k+l=2n present

h+k+l=2n+1 extincted

μ_{Ni} || **c.** AFM spirals

χ^2=1.55

Bad χ^2=2.7

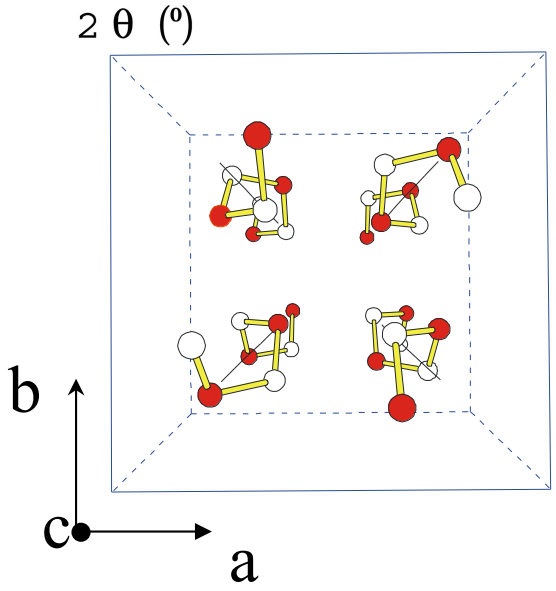

Spin Configurations

$I4_1cd$ sp.gr., 16 Ni^{2+}

√I. AF-chains (spirals) 2. F-chains (spirals)

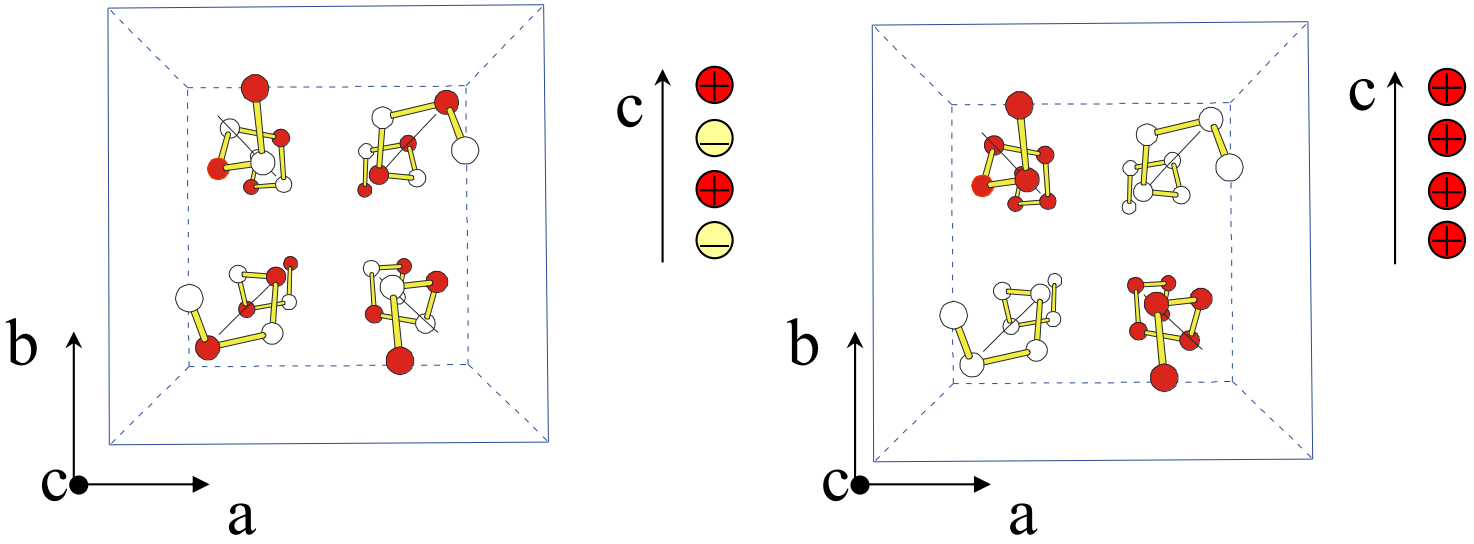

Arrangements of spirals

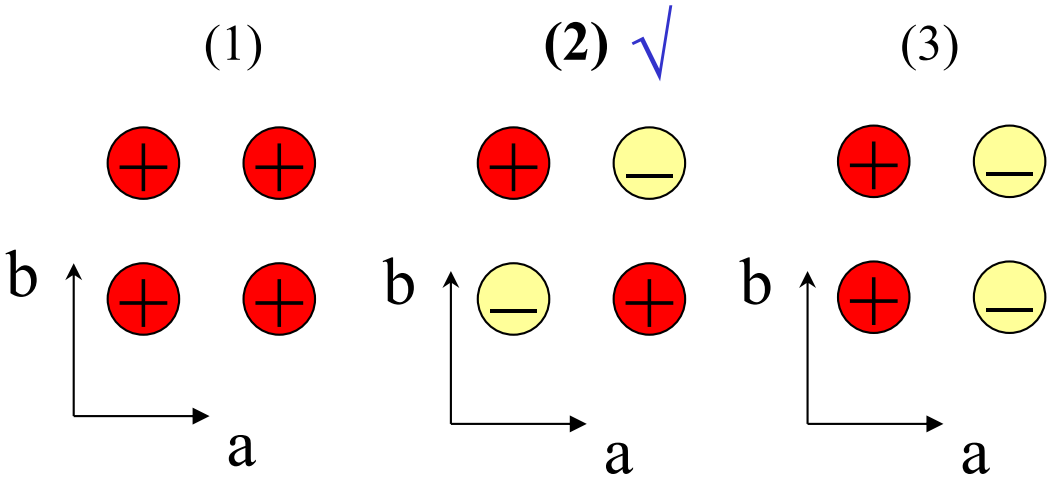

III. Helix structure (90° spin rotation along the spiral)

Spin direction in AFM chains

Illustration of sensitivity to the magnetic moment direction.

AF-chains, μ_{Ni} || (**ab**) type 2.
Wrong direction → bad χ^2=2.05.

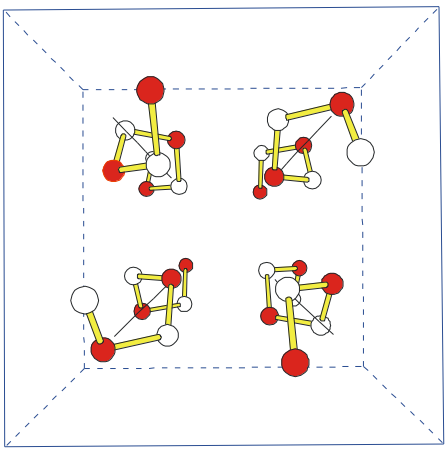

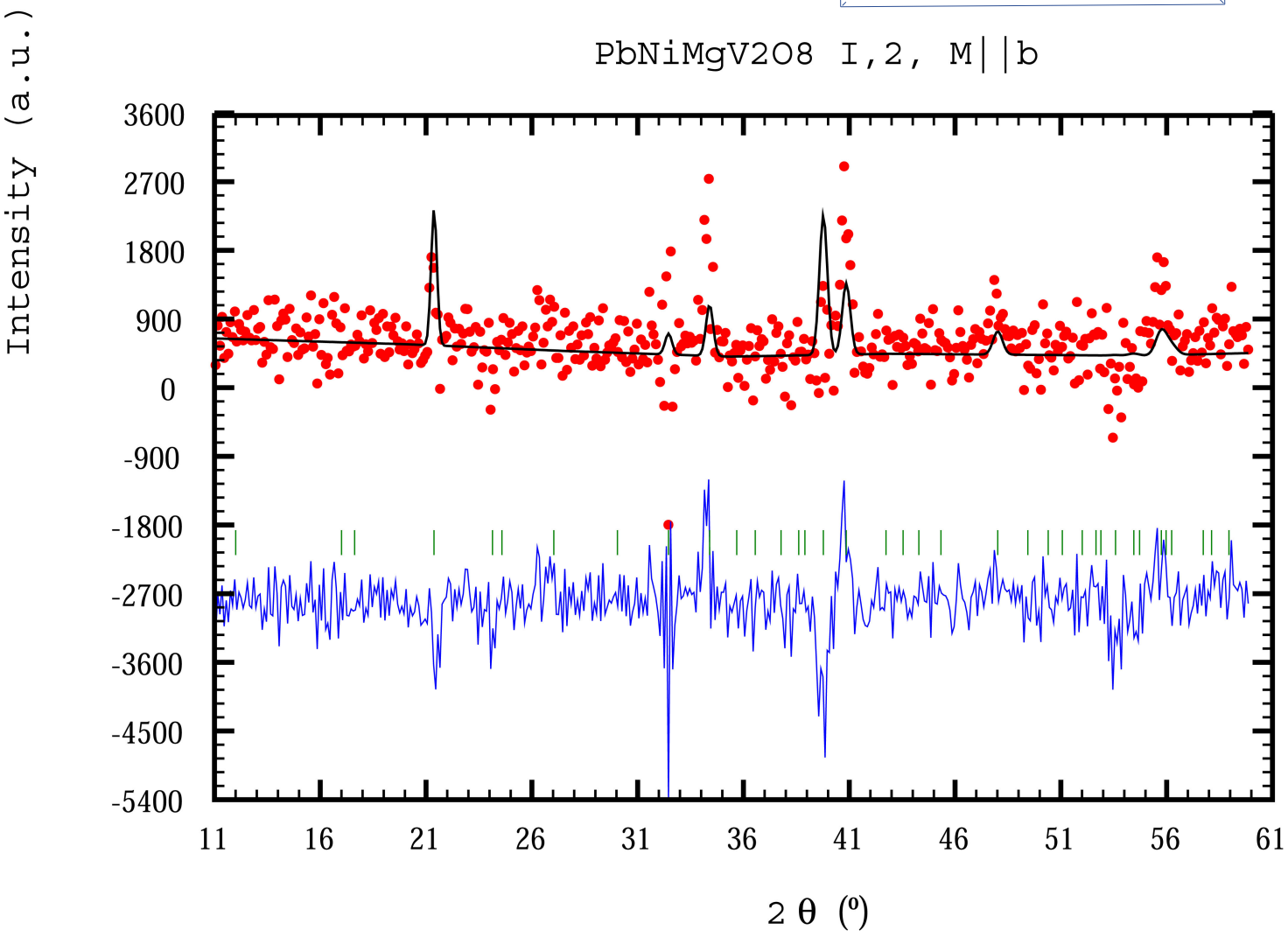

Examples of “wrong” AF-spiral configurations

Theoretical profiles calculated for the same moment (scale factor) obtained from refinement to the “right” spin arrangement.

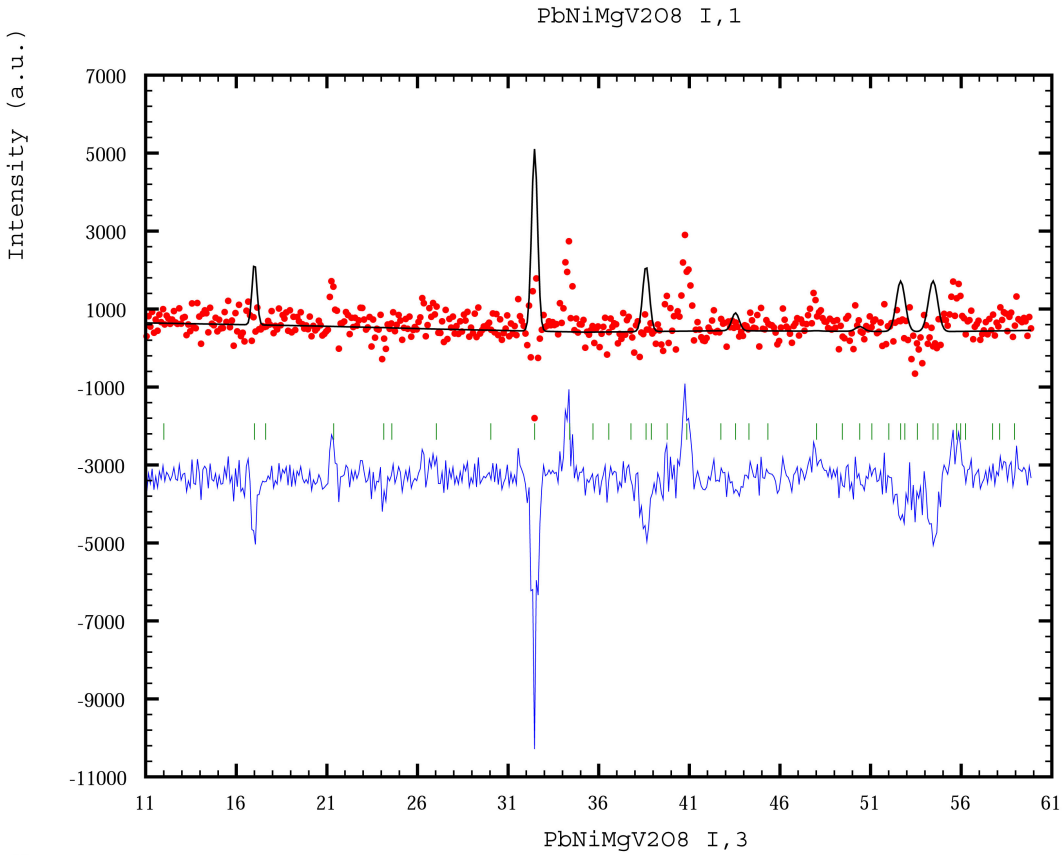

(1)

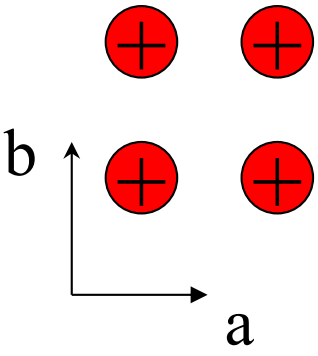

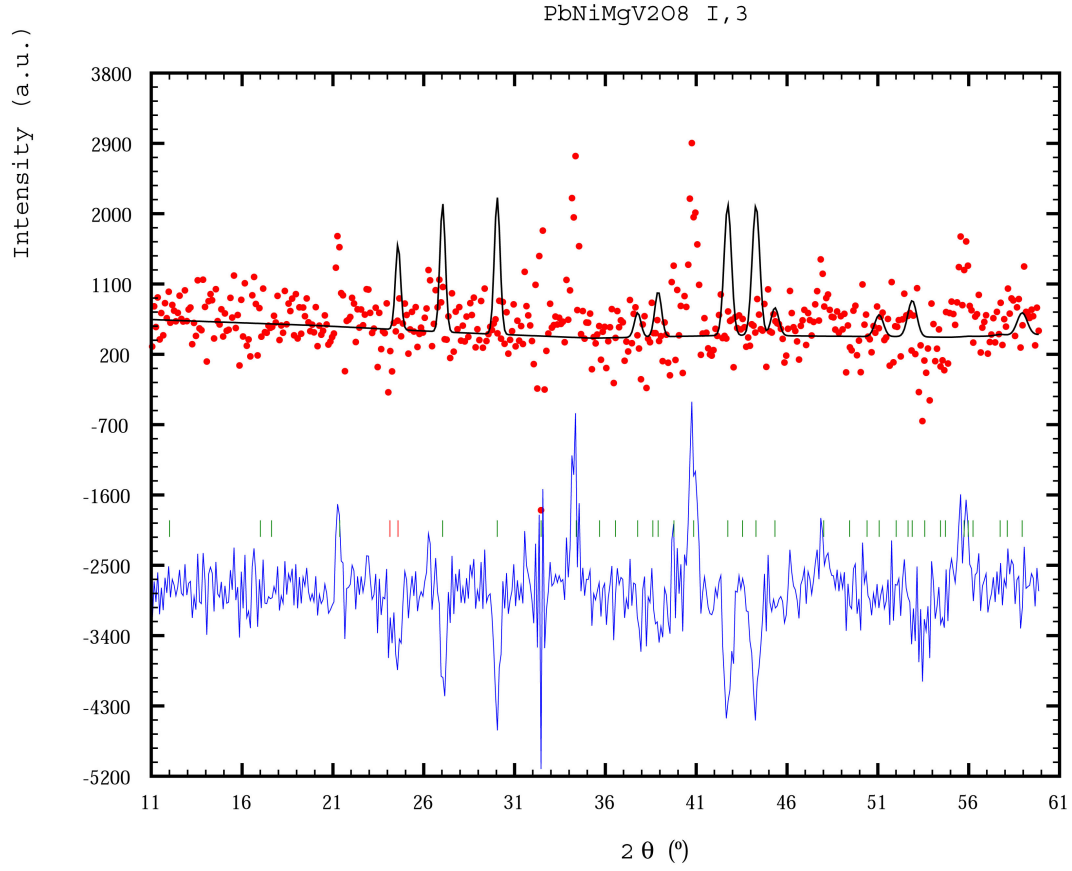

(3)

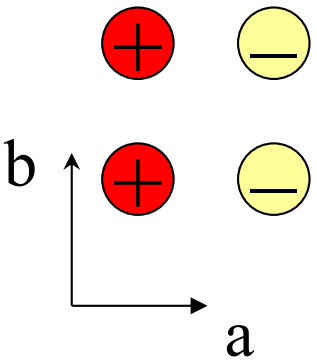

FM-canting of spins

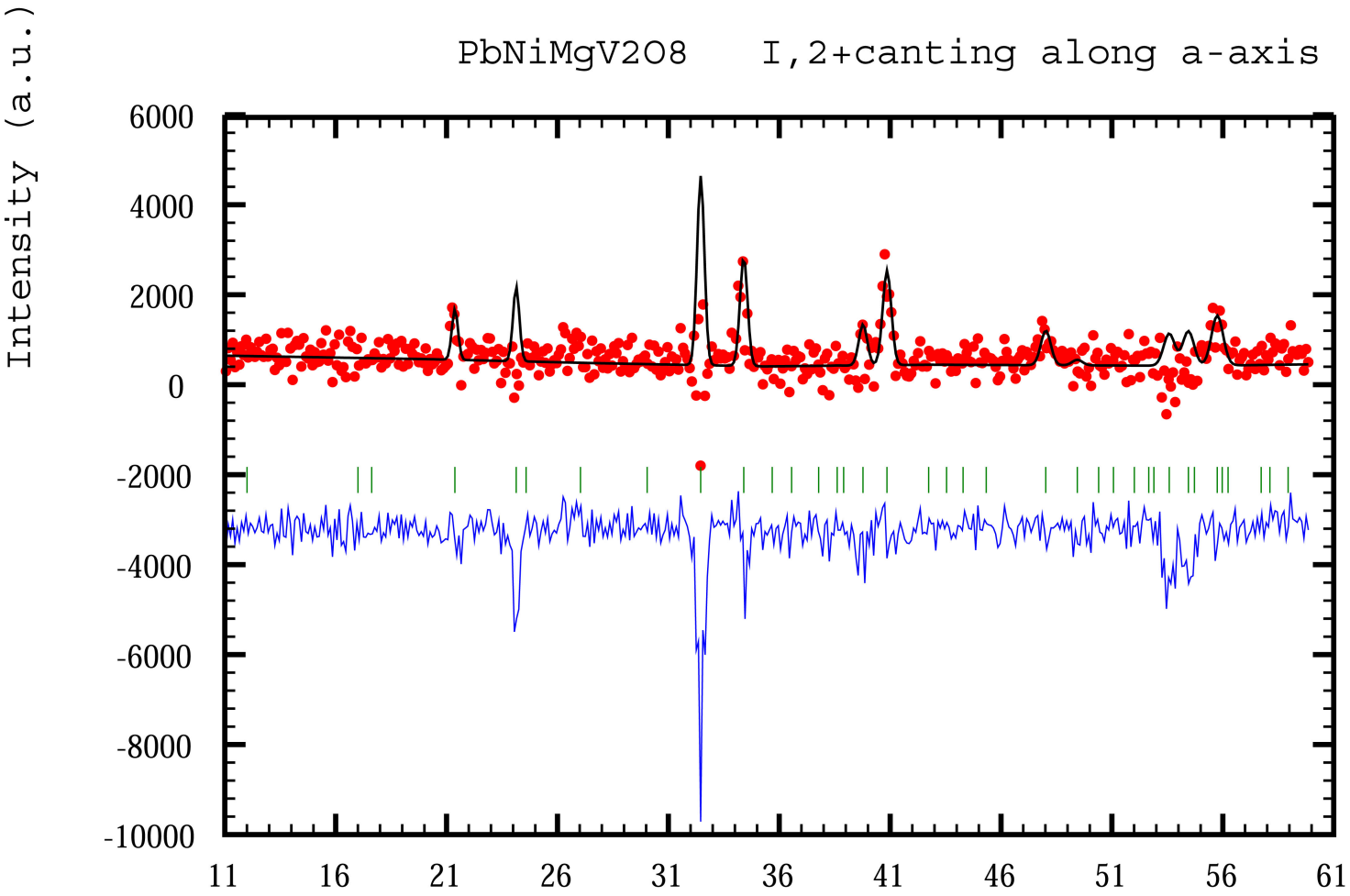

Pattern calculated assuming a FM component along the [100] direction and a moment size equal to half of that found for the purely AF spin AF-chains

statistical estimate of the canting component $\mu_x \sim (0.03 \pm 0.19)\ \mu_z$.

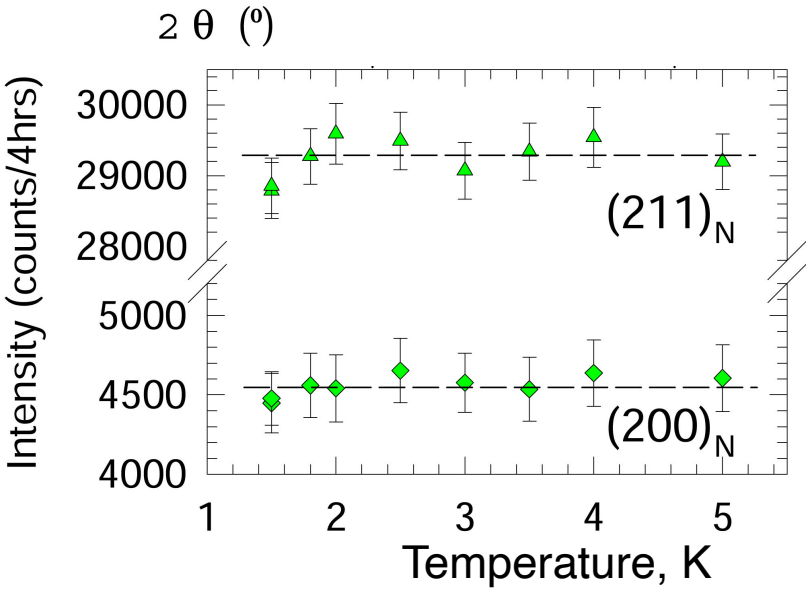

T-dependence of the integrated Bragg peak intensities

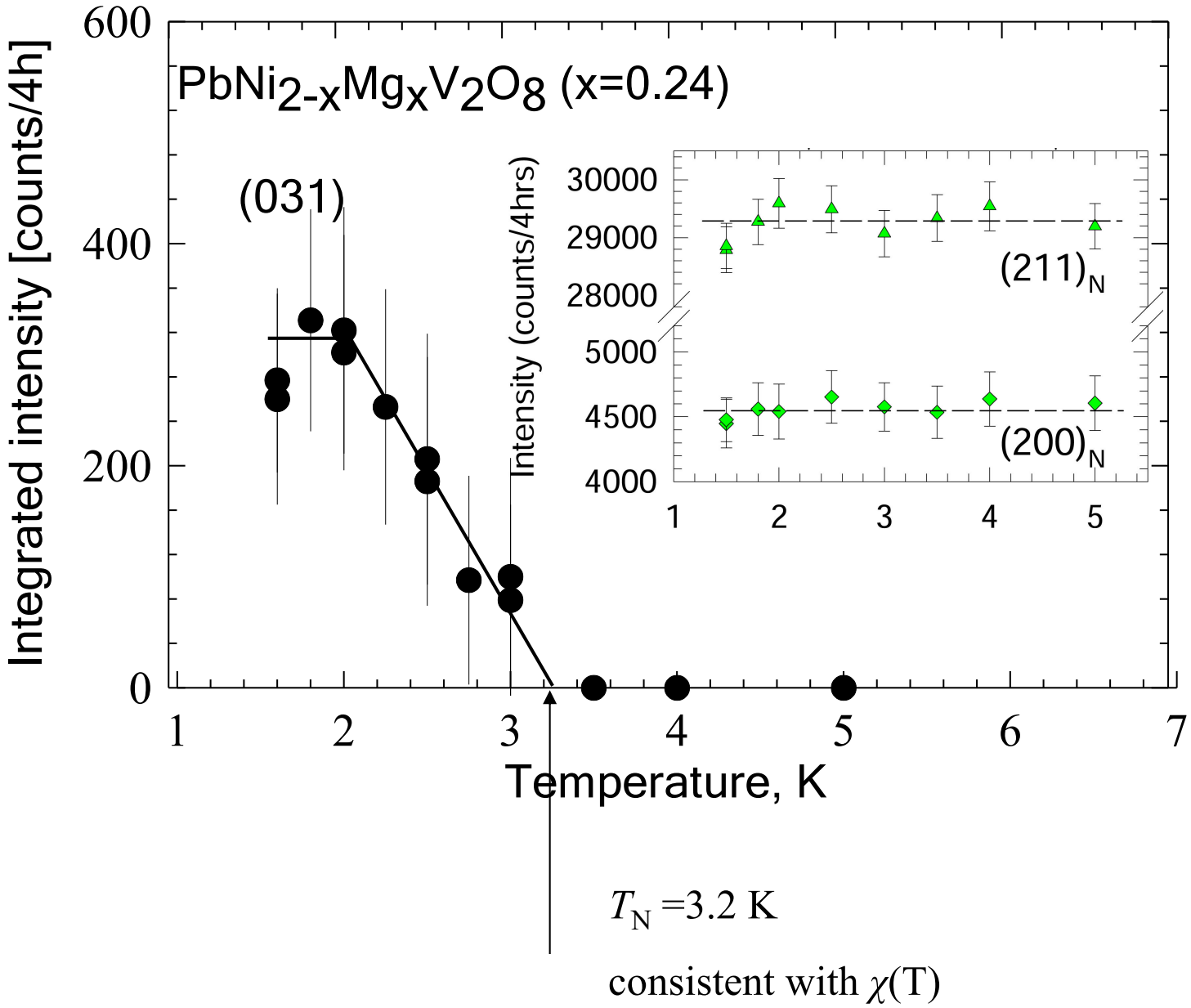

Magnetic Structure of $PbNi_{2-x}Mg_xV_2O_8$ (x=0.24)

Refined magnetic moment is 0.9(1) μ_B per Ni-site, at 2 K.

Local magnetic structure
- 2×x(=0.48) spin-vacancies
- end-chain Ni can carry [1.76/0.48]×0.9= 3.3 μ_B.
- Spin-½ value 1.73 μ_B

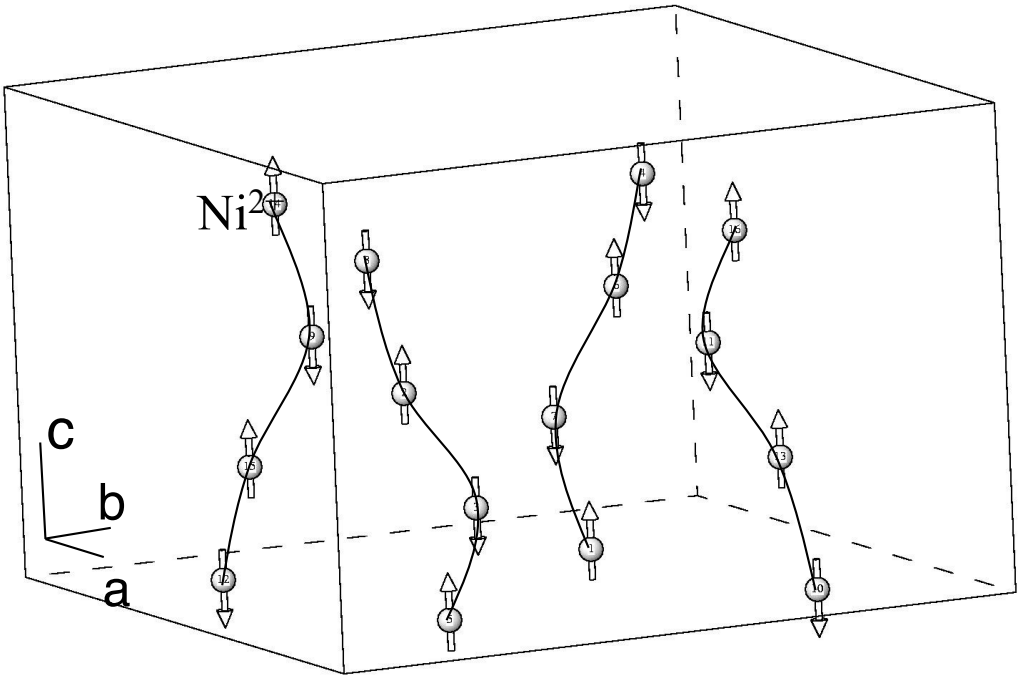

Chain length $\langle L \rangle = (2/x) \cong 8$

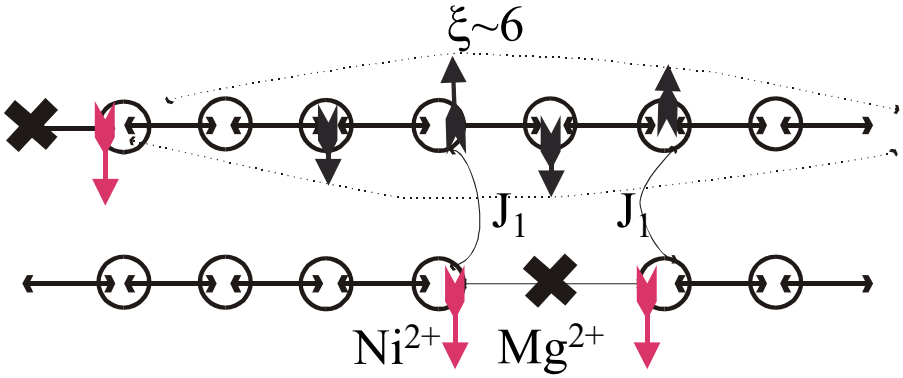

ZF-μ⁺SR spectra was a convolution of more than one muon local fields (H_{int}). These internal fields take a number of values, $\langle H_{int} \rangle \sim$ 30, 120, 220 G. /A.Lappas et al., unpublished (2001)/

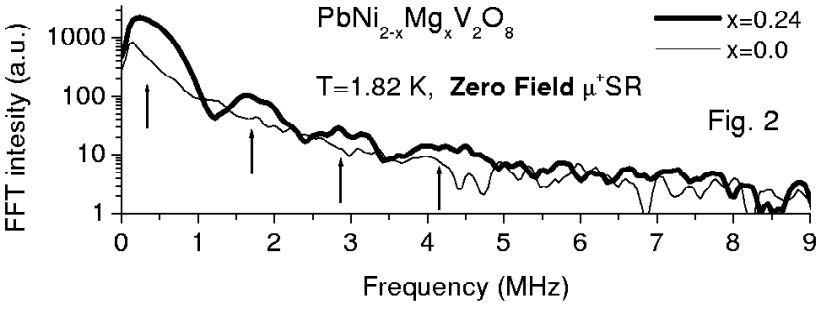

Conclusions

1. Phase diagram $T_N(x)$ of $PbNi_{2-x}Mg_xV_2O_8$, $0.04 \leq x \leq 0.24$ is confirmed: T_N is increasing rapidly, rising to a maximum at an optimum Mg-doping level of x=0.12.
2. Neutron diffraction in the $PbNi_{1.76}Mg_{0.24}V_2O_8$ probes an average ordered moment size of 0.9(1) μ_B per Ni-site, at 2 K. The moments are antiferromagnetically coupled below T_N=3.2 K, both in the chains along the c-axis and within the same (ab)-plane for Ni-sites on nearest-neighbour chains
3. Below T_N, the x=0.24 Mg-rich compound exhibits metamagnetic behaviour. $H_c(T=0K)$=1.2T.

Published: 16 July, 2002 https://doi.org/10.1103/PhysRevB.66.014428
Magndata PbNi1.76Mg0.24V2O8 (#0.1035) BNS, Bilbao